Journal of Materials Chemistry A

Poly-Functional Porous-Organic Polymers to access Functionality–CO2 Sorption Energetics Relationships

Journal:	*Journal of Materials Chemistry A*
Manuscript ID:	TA-ART-07-2015-005297.R1
Article Type:	Paper
Date Submitted by the Author:	06-Aug-2015

Complete List of Authors:	Alkordi, Mohamed; Zewail City of Science and Technology, Center for Materials Science Haikal, Rana; Zewail City of Science and Technology, Center for Materials Science Hassan, Youssef; Zewail City of Science and Technology, Center for Materials Science Emwas, Abdul-Hamid; King Abdullah University of Science and Technology,, ano-Catalysis Laboratory (KAUST NanoCat), KAUST Catalysis Center (KCC), Belmabkhout, Youssef; King Abdullah University of Science and Technology, Chemical science

SCHOLARONE™
Manuscripts

Table of Contents artwork here

Poly-Functional Porous Organic Polymers are constructed to probe the effect of chemical functionality on the observed Q_{st} for CO_2.

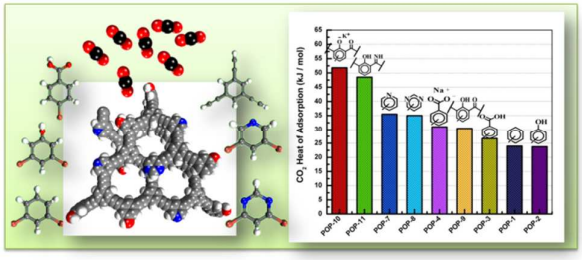

Journal Name

ARTICLE

Received 00th January 20xx,
Accepted 00th January 20xx

DOI: 10.1039/x0xx00000x

www.rsc.org/

Poly-Functional Porous-Organic Polymers to access Functionality–CO_2Sorption Energetics Relationships

Mohamed H. Alkordi,*[a]Rana R. Haikal,[a]Youssef S. Hassan,[a] Abdul-HamidEmwas[b], and Youssef Belmabkhout[c]

Herein, we report a facile approach towards construction of Poly-Functional Porous Organic Polymers (POPs). The functional groups employed were selected to span the range of Lewis-base, neutral, to Lewis-acid character. Our results underline the effect of chemical functionality on the observed Q_{st} for CO_2 adsorption inside the material, being largest for functional groups with electron donating O- and N-centered Lewis base sites. Our systematic investigation within a family of POPs revealed a wide range for CO_2 heat of adsorption(23.8~53.8 kJ/mol) that is clearly associated to the chemical nature of the functional groups present. In addition, post synthetic modification on POPs reported herein demonstrated a facile pathway to dramatically enhance carbon dioxide uptake energetics.

Introduction

Among porous solids, metal-organic frameworks (MOFs) and Porous-Organic Polymers (POPs) continue to receive considerable scientific interest due to their wide range of potential applications in current demanding technologies.[1] Porous solids, in general, are amenable to bottom-up assembly from judiciously designed molecular building blocks (MBBs) into a desired framework expanding and/or decorating a specific blueprint network topology.[2] POPs are an emerging class of polymeric materials accessible through covalent linkage of pre-selected MBBs. POPs commonly exhibit rigid structures, high thermal and chemical stabilities, low densities, and in certain cases permanent porosity with specific surface areas surpassing those of well-known zeolites and porous silicates.[3] Recent reports outlined several synthetic pathways to construct POPs including, but not limited to: (i) boronic acid condensation, (ii) imine formation, (iii) Sonogashira-Hagihara cross-coupling, (iv) triazine synthesis via nitrile trimerization, and (v) cobalt-catalyzed acetylene trimerization.[4] Common to the aforementioned bond-making reactions is irreversibility under the reaction conditions used (with exception of imines and boranes), rendering isolation of crystalline POPs challenging. On the other hand, solvothermal syntheses of MOFs utilize the reversibility of coordination bonds to access highly crystalline materials. Crystallinity in MOFs is key towards structure-function relationship investigations that permit tailoring materials towards specific applications. [2a]In absence of information encoding at the molecular level and due to reversibility of coordination bonds under solvothermal conditions, MOFs with most symmetric structures are commonly isolated.[5] However, utilizing the directionality and rigidity of judiciously selected building blocks permit access to non-default topologies. Accordingly construction of MOFs based on unitary and binary nets are frequently reported, while assembly of MOFs of higher hierarchy remain challenging.[6] In addition, diversifying the chemical functionalities within a particular solid is of particular interest. Yaghi and co-workers have successfully attempted to increase the number of functionalized organic linkers, present simultaneously, in a family of crystalline solids termed multivariate MOFs (MTV-MOFs).[7]However, it was previously generally accepted that such attempts will lead to either amorphous solids or, at best, mixed phases of mixed units. Hence, attempts to explore and extend the solid state chemistry into the realm of the all-organic, porous, polymers are of high interest. Attempts to introduce mixed MBBs into the assembly of POPs are of interest due to the different types of applications that can be accessed utilizing polyfunctional materials. Herein, we report a facile approach towards construction of POPs from the trigonal-planar

[a]Zewail City of Science and Technology. Center for Materials Science. Sheikh Zayed District, 12588, Giza, Egypt. E-mail: malkordi@zewailcity.edu.eg.
[b]King Abdullah University of Science and Technology (KAUST), NMR Core lab, Thuwal, 23955-6900 KSA.
[c]King Abdullah University of Science and Technology (KAUST), Center for Advanced Membranes and Porous Materials, Thuwal, 23955-6900 KSA.

Electronic Supplementary Information (ESI) available: [details of any supplementary information available should be included here]. See DOI: 10.1039/x0xx00000x

This journal is © The Royal Society of Chemistry 20xx

triethynylbenzene nodes and functionalized linkers with a wide range of functional groups. In certain examples, we have demonstrated that more than one functional linker can be incorporated into the backbone of porous solids.

Of interest to material designers is the ability to fine tune a platform material to address specific applications. One pathway towards this goal, among others, is framework decoration. Essential for successful framework decoration is utilization of functional auxiliary groups that don't interfere with the bond-making process, necessary to construct isostructural solid materials with tuned functionality.[2a] In this report, we demonstrate the versatility of a Sonogashira-Hagihara cross-coupling reaction to construct a family of porous solids with wide range of functional groups, namely pyridine, pyrimidine, phenol, ketophenols, and aromatic carboxylic acid. This approach utilizes the nearly similar reactivity of several brominated aromatic molecular building blocks towards the C–C heterocoupling reactions utilized. Accordingly, a family of POPs could be constructed containing one or multiple type(s) of chemical functionalities simultaneously integrated in the backbone of the solids. Porous polymers containing myriad of functional groups are of particular interest, especially towards applications in CO_2 capture, gas separation, heterogeneous catalysis, and most recently catalytic photoelectrochemical water splitting.[8] It is of particular interest to experimentally assess the performance of such generated POPs when the backbone is maintained while functionality can be controllably mixed or interchanged. Cooper and co–workers have detailed certain parameters significant to formation of POPs through Sonogashira-Hagihara cross-coupling, in which the solvent system of N,N`–dimethylformamide (DMF) and triethylamine (Et_3N) contribute positively to the degree of porosity of the isolated solids.[9] Due to the irreversible C–C bond formation step, POPs constructed through cross-coupling reactions are widely amorphous solids,[10] precluding solution-based structure characterization and making structural characterization through diffraction techniques particularly challenging. However, a wide range of structural characterization techniques including IR and solid–state NMR spectroscopy, gas sorption, elemental analysis, and thermogravimetric analysis techniques can draw more detailed picture for the chemical composition of the solids.

Results and Discussion

Reactions of 1,3,5-triethynylbenzene, as a tritopic node, and *m*–dibromobenzene derivatives, as angular linkers, in a mixture of DMF/Et_3N in presence of catalysts and under inert atmosphere at 80°C resulted in porous organic polymers POPs 1-8, **Scheme 1**. In one particular example, reaction of 4,6-dibromopyrimidine, 3,5-dibromophenol, 3,5-dibromopyridine, and 1,3,5-triethynylbenzene under Sonogashira-Hagihara cross-coupling conditions resulted in deep-brown solid, POP-5, **Figure 1**. The successful simultaneous assembly of the four selected MBBs into POP-5 was evidenced from attenuated total reflectance Fourier-transform infrared (ATR-FTIR) spectroscopy. Linkage through alkyne groups is evident from absence of the characteristic terminal alkyne ν_{C-H} band (3272 cm^{-1}) attributed to the reactant 1,3,5-triethynylbenzene and detectable shift of alkyne $\nu_{C\equiv C}$ stretching (from 2112 cm^{-1} in triethynylbenzene to 2204 cm^{-1} in POP-5, similar behavior was observed for all reported POPs, see SI). Presence of additional

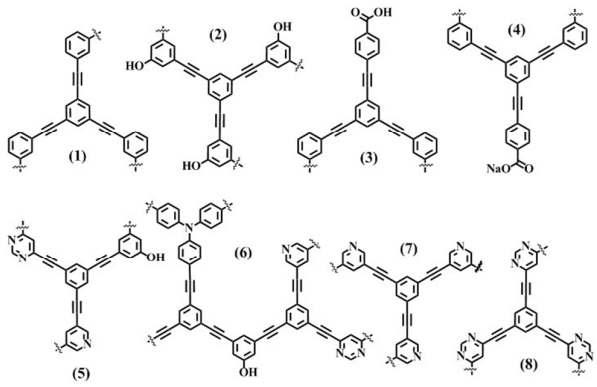

Scheme 1. Schematic illustration of possible repeat units in POPs 1-8.

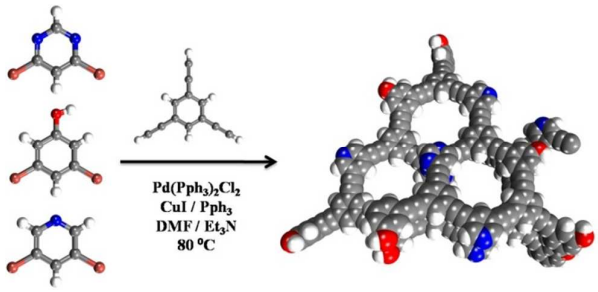

Figure 1. Synthesis strategy for POP-5 with a structural model of a potential oligomer chain. Carbon (grey), oxygen (red), nitrogen (blue), hydrogen (white).

IR spectroscopic markers including broad ν_{O-H} stretching band centered at 3300 cm^{-1} and $\nu_{C=N}$ stretching at 1560 cm^{-1} further support incorporation of the phenol and N-containing heterocycles into the isolated solid. Additional IR markers include the carbonyl absorption band, $\nu_{C=O}$ at 1716 cm^{-1}, and aromatic ketone absorption band, $\nu_{C=O}$ at 1653 cm^{-1}(see SI for FTIR spectra for POPs reported here).

To further probe the structures of the prepared solids, solid–state NMR spectra were collected and indicated presence of the aforementioned functionalities as inferred from their characteristic chemical shifts (SI). The ^{13}C CPMAS-NMR spectrum of POP-1 indicated internal alkyne (δ = 89.3 ppm) and aromatic carbons (δ = 123.4 ppm for tertiary carbons connected to the alkyne bond, δ = 129.6 ppm for secondary C-H carbons). The relatively narrow peaks at 89.3 ppm and 123.4 ppm indicated relatively homogenous internal alkyne environment, a marker taken to indicate reduced polymer dispersity. The ^{13}C CPMAS-NMR spectra for the rest of POPs reported herein maintain similar patterns as in POP-1 but with the extra, expected peaks at chemical shifts corresponding to the functional groups present. In POP-2, the NMR spectrum indicated internal alkyne (δ = 91.2 ppm) and aromatic carbons (δ = 125~137 ppm for secondary and tertiary carbons) as well as the aromatic phenol (δ = 157.8 ppm). In POP-3, the NMR spectrum indicated internal alkyne (δ = 90.12 ppm) and aromatic carbons (δ = 123~136 ppm for secondary and tertiary carbons) as well as the aromatic carboxylic carbon (δ = 164.9 ppm). In addition, residual peaks were observed at the aliphatic region (δ = 13.56, 60.81 ppm), indicating residual ester groups left after the post-synthetic hydrolysis step. In POP-4, the NMR spectrum indicated internal alkyne (δ = 89.49

This journal is © The Royal Society of Chemistry 20xx

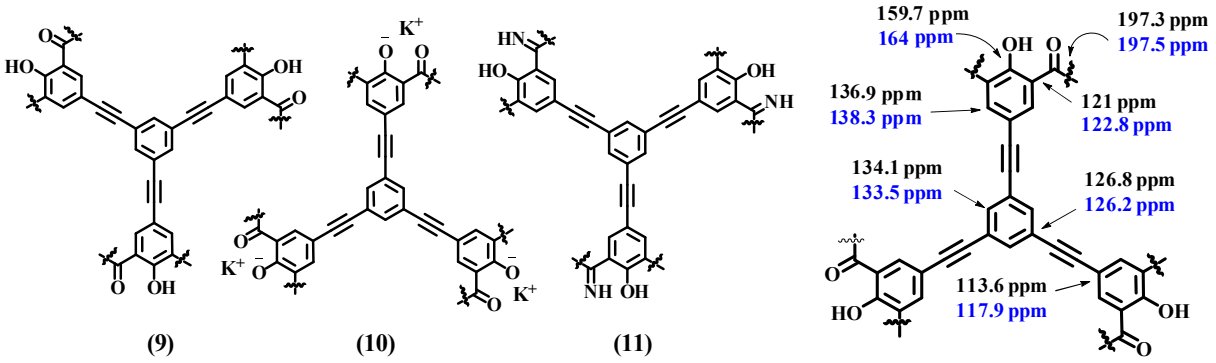

Figure 2. (left) Proposed structure for POPs 9-11 with calculated (black) and observed (blue) solid-state NMR chemical shifts for POP-9 (right).

ppm) and aromatic secondary and tertiary carbons (δ = 123~136 ppm), as well as the aromatic carboxylate carbon (δ = 168.5 ppm). The NMR spectrum of POP-5 indicated two distinct chemical shifts for the internal alkyne (δ = 90.9, 81.1 ppm) in agreement with expected chemical shifts for the asymmetric internal alkyne groups. It is expected for the alkyne carbons connected to the more electron-rich heteroaromatic rings (pyridine and pyrimidine) to experience upfield chemical shift relative to the alkyne carbons connected to the central tri-substituted benzene ring. In addition, the NMR spectrum for POP-5 showed peaks for aromatic carbons (δ = 123~135 ppm for secondary and tertiary carbons) as well as the aromatic pyridine C-H carbons at the α–position (δ = 149.8 ppm) and the phenol carbon (δ = 157.5 ppm). The C-H carbons at position 2 on the pyrimidine ring are expected at δ = 159 ppm, and thus can't be easily deciphered from the phenolic carbon peak. Similarly, POP-6 exhibited similar NMR pattern as POP-5 with the expected difference for the N-connected aromatic carbons peaks in triphenylamine spacer. Indeed, chemical shifts for the N-connected carbon atoms appear as a shoulder on the peak assigned for the aromatic pyridine C-H carbons at the α position (δ = 149.8 ppm, calculated 148 ppm). For POP-7, the NMR spectrum indicated two distinct chemical shifts for the internal alkyne (δ = 92.1, 87.6 ppm) in agreement with expected chemical shifts for the asymmetric internal alkyne groups as discussed previously. In addition, the NMR spectrum for POP-7 showed peaks for aromatic carbons (δ = 123~135 ppm for secondary and tertiary carbons) as well as the aromatic pyridine C-H carbons at the (α) position (δ = 150.2 ppm) and the C4 carbon atoms of the pyridine ring (δ = 135.6 ppm, calculated at 140.4 ppm). For POP-8, the NMR spectrum exhibit two distinguishable chemical shifts for the internal alkyne (δ = 88.6, 80.3 ppm) in agreement with expected chemical shifts for the asymmetric internal alkyne groups. In addition, the POP-8 NMR spectrum showed peaks for aromatic carbons (δ = 121.6 and broad peak at ~135 ppm for secondary and tertiary carbons, respectively). Moreover, a peak was observed at (δ = 149.1 ppm) and assigned to the aromatic pyrimidine tertiary C-4,6 atoms (calculated at 154 ppm). In addition, a distinct signal was observed for the carbons at position 2 on the pyrimidine rings (δ = 158.4 ppm, calculated at 159.4 ppm). For POP-9, **Figure 2**, the NMR spectrum indicated a peak characteristic of the internal alkyne (δ = 90.8 ppm) as well as five distinct peaks at the aromatic range (117.9, 122.8, 126.2, 133.5, 138.3 ppm), in agreement with the proposed structure (calculated 113.6, 121, 126.8, 134.1, and 136.9 ppm). The aromatic phenol character

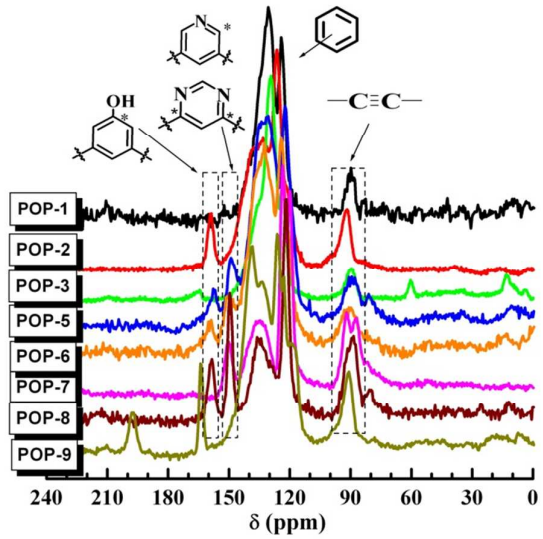

Figure 3. 13C-CPMAS-NMR spectra for selected POPs.

is evident from the peak observed at 164 ppm (calculated ~159.7 ppm). Moreover, the presence of bridging ketones in benzophenone-like repeat units is evident from the peak observed at 197.5 ppm (calculated 197.3 ppm). Superposition of the ^{13}C-CPMAS-NMR spectra, **Figure 3**, facilitate identification of chemical shifts corresponding to the overall similar backbone structures, as well as help identifying variance due to different functionalities present. The synthesized POPs exhibit high thermal stability (up to ca. 300 °C) as confirmed by thermogravimetric analysis (SI). In addition, chemical stability in heated base and acid solutions was demonstrated for POPs-3,4. Incubation of the ester-derivative of POP-3 in sodium hydroxide solution at 85°C for 24h resulted in the targeted ester hydrolysis. The resulted sodium salt of the carboxylic acid was easily transformed, post-synthetically, into the conjugate acid through incubation in 1M HCl solution at 85°C for 3h. Both the free-acid form, POP-3, and the sodium salt POP-4, exhibit nearly identical surface area and shape of N_2 sorption isotherms, yet confirming their overall structural integrity upon treatment with heated acid and base solutions.

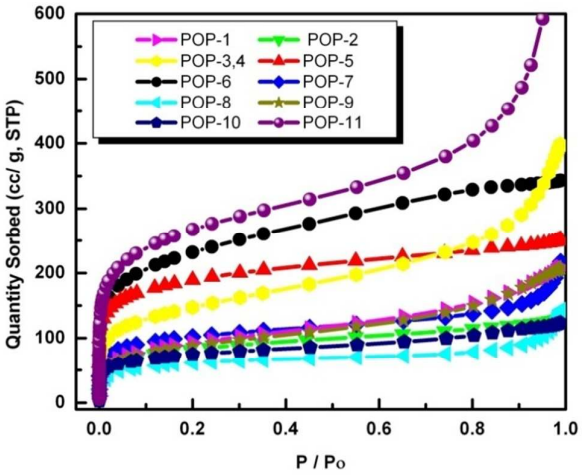

Figure 4. N_2 gas adsorption isotherms for **POPs 1-11**

In order to assess the porosity of POPs reported here, nitrogen sorption isotherms were collected at 77.3 K, **Figure 4**. The measured isotherms were found to exhibit type I–like isotherms where most of the constructed POPs exhibit H_2–type desorption hysteresis, following the IUPAC classification. This behavior can be more likely associated with the occurrence of swelling, commonly observed in POPs[11], or originating from interparticle voids.[12]Indeed, most materials reported herein exhibit significant volume shrinkage upon loss of solvent during the degassing process prior to isotherm measurements. For POPs 1-11 the estimated apparent Brunauer–Emmett–Teller (BET) surface areas and total pore volumes are reported in **Table 1** (please refer to SI for pore volume distribution plots). POPs-10,11 are the result of post-synthetic modification (PSM) of POP-9.It is interesting toobserve a slight decrease in surface area upon metallation with potassium ions (POP-9 to POP-10) while observing an appreciable increase in surface area upon treatment with methanolic ammonia (POP-9 to POP-11). This observation can potentially be explained in terms of induced structural changes upon metallation and amination. It is plausible to presume interplanar and/or inter-chain shrinkage after metallation due to chelation of potassium ion intercalated between the polymer layers/chains. However, in case of amination, an interplanar/inter-chain hydrogen bond interactions can potentially cause restructuring of the polymer and in turn inducing swelling to maximize interplanar/ inter-chain H-bond interactions. The functionalities in the POPs reported herein were carefully selected, *a priori*, in order to ascertain the chemical composition-adsorption energetic relationships in solid–CO_2 interactions. The POPs of interest were selected to incorporate various functional groups of different chemical nature, such as the (i) Lewis base phenoxide, carboxylate, pyridine, and pyrimidine, (ii) the neutral benzene ring, (iii) the weakly acidic phenol, (iv) the Lewis acid carboxyphenyl group, and (v) the mixtures thereof. CO_2 sorption isotherms for POPs 1-11 were measured (SI). It is noticeable that the majority of POPs adsorb similar amounts of CO_2at 1 bar (in the range of 19~22 cc/g) due to mainly the similarity in surface area. In agreement with this observation, an increased total CO_2 uptake was noticed for the extended POP-5 and POP-6 (27-30 cc/g). Furthermore, comparing CO_2 uptake for the POPs 9 and 11 (increase from ~ 20 to ~45 cc/g, respectively for isotherms measured at 283K) indicates a proportionality relationship between surface are and total uptake.Variable temperature isotherm measurements were conducted for POPs 1-11 and Q_{st} was calculated for each material. Isosteric heat ofadsorption for CO_2 in a particular porous solid gives a clear indication on the affinity of CO_2.to the porous solid which in turn can (i) determine the adsorption selectivity towards CO_2 and (ii) can indicate the required energy to regenerate the solid after sorption of CO_2. Q_{st} for CO_2 in POPs are usually in the range of 15–25 kJ mol^{-1} for non-functionalized materials, and mainly driven by the effect of pore size and driven by pore filling.[13] Chemical functionalization, especially amine grafting, of POPs is of interest to enhance their CO_2 adsorption energetics.[14] Eddaoudi and co–workers have recently reported a facile approach to post–synthetically modify an aldehyde–containing POP through anchoring of free primary amine, resulting in enhanced Q_{st} for CO_2 adsorption.[15] The calculated Q_{st} values for CO_2 adsorption in POPs 1-8, **Figure 5**, were found to be within the range of 23.8–35 kJ/mol and exhibit an interesting behavior associated with the type of chemical functionality present inside each POP. Inspection of the Q_{st} values obtained for POPs 1-8, particularly at low CO_2 loading, revealed a systematic tendency towards stronger CO_2–solid interactions within POPs containing Lewis-base sites. The pristine POP-1 (Q_{st} ~ 24 kJ/mol) contains the non-substituted benzene ring as the ditopic linker and thus was utilized as the reference point in this study. Introducing the phenol functionality in POP-2 did not seem to positively impact the heat of adsorption of CO_2 (Q_{st} ~ 23 kJ/mol) as compared to the pristine POP. Substitution with carboxylic free acid groups in POP-3 did slightly enhance the heat of adsorption (initial Q_{st} ~26.7 kJ/mol) but, overall, remains with similar pattern as the non-functionalized POP-1. In POP-4 we opted to study the effect of transforming the free carboxylic acid form into its conjugate base. The sodium benzoate in POP-4 was found to significantly enhance its affinity towards CO_2, (Q_{st} range from 31~21 kJ/mol over the range of coverage studied). We then attempted to study the interactions within a multi-component solid, POP-5. Substituting pyridine and pyrimidine rings for part of the phenol-based monomers resulted in a mixed functionality POP-5 with enhanced CO_2 interactions (Q_{st}~30.3 kJ/mol). Increasing the pore size dimensions through incorporation of the extended triphenylamine linker in POP-6 was found to cause decreased, although slight, CO_2 adsorption interactions (Q_{st} ~ 28.9). This is to be expected due to weakening of synergistic effects of polar and/or polarizable groups interacting with adsorbed CO_2 molecules inside the pores of a POP. Indeed, the observed Q_{st} for POPs-5,6 reflects the effect of mixed functionality nature of the polymer, falling midway between the ranges observed forphenol–based and N–heterocycle based POPs.

POP	1	2	3	4	5	6	7	8	9	10	11
BET S.A (m^2/g)	332	293	532	532	687	830	356	215	316	259	846
P.V (cc/g)	0.31	0.199	0.6	0.6	0.38	0.53	0.31	0.2	0.31	0.19	0.78

Table 1. BET surface area and pore volume values for POPs 1-11.

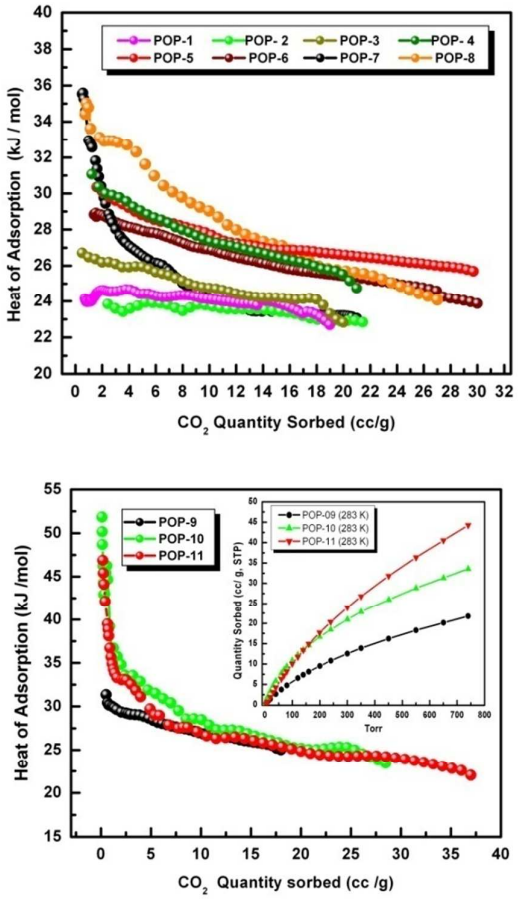

Figure 5. Heat of adsorption plots for CO_2 gas into POPs **1-8** (top)and POPs **9-11**(below) with insert showing CO_2 uptake at 283K.

The highest Q_{st} values were observed for POP-7 and POP-8 (~35 kJ/mol) and can be attributed to abundance of N-donor sites inside the pyridine and pyrimidine-containing POPs, respectively. The steeper decrease of Q_{st} for the pyridine-based POP-7 can be attributed to the lower abundance of N-donor sites, as compared to the number of such sites in the pyrimidine-based POP-8. In POPs 9-11, **Figure 5**, the poly-ketophenol character ensures abundance of Lewis acid and base sites within the pores of the solids. The observed CO_2 heat of adsorption in the pristine POP-9 was found to be both relatively high (~ 30 kJ/mol) and uniform over the whole coverage, indicating uniformity of adsorption sites distribution within POP-9. Post-synthetic modification (PSM), simply through incubation in heated alkali base solution, was found to be sufficient to deprotonate the acidic phenol protons to result in POP-10. The phenoxide functionality in POP-10 was found to result in significant enhancement of CO_2 heat of adsorption. POP-10, by far, showed the highest Q_{st}(~ 51 kJ/mol) among the porous solids investigated herein. This can rationally be justified based on abundance of Lewis base sites in the deprotonated, pheoxide-containing polymer. Moreover, similar PSM of POP-9, incubation under heated methanolic ammonia solution, resulted in the imine-derivative, POP-11. The imine functionality in POP-11 was found to positively affect CO_2 heat ofadsorption at low coverage, measured Q_{st} (~48 kJ/mol). This observation can rationally be justified based on abundance of Lewis base imine-sites that can interact favorably with sorbed CO_2 molecules.

In this report, we have experimentally demonstrated a noticeable trend in increasing/controlling the energetics for

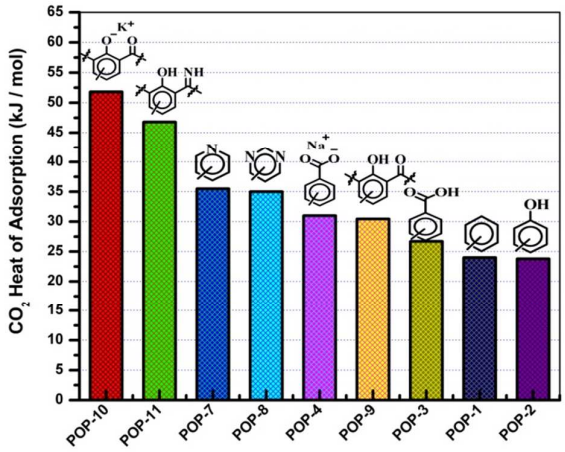

Figure 6. Functional groups and initial heat of adsorption of CO_2 in POPs 1-11

CO_2 adsorption in a family of POPs, that is associated with the nature of binding sites inside the porous solids, **Figure 6**. This observed Q_{st} trend clearly indicate an underlying relationship between Lewis base character of the binding site and its affinity towards CO_2. Phenoxide alkali metal salt, imine, N-containing heterocycles, and alkali salt of aromatic carboxylate, were all found to be desirable candidates to incorporate into the chemical composition of CO_2-capturing porous solids. Closer look into the observed Q_{st} values suggests that N-donor Lewis base sites (in POPs 7,8) can interact more favorably with CO_2 molecules as compared to the more electronegative oxygen atoms in carboxylate-based POP-4. In conclusion, we presented a facile approach to construct functionalized POPs with functional groups spanning the range of Lewis-base to neutral to Lewis-acid character. We have also demonstrated the effect of the nature of chemical functionality on the observed Q_{st} for CO_2 adsorption inside the material. In addition, it is demonstrated that increasing the dimensions of the pores inside the material, while maintaining the chemical composition, resulted in decreased enthalpy of interactions. It is suggested that incorporating the above factors, Lewis-base functionality and small pores system, into designer materials can potentially result in materials with favorable CO_2 uptake energetics. Materials with high chemical and thermal stability (preferably all-organic) that simultaneously incorporate Lewis-base sites and small pore volumes are of particular potentials to address current challenges in CO_2 separation and capture.

Experimental

For detailed synthesis procedures and characterization including FT-IR, gas sorption isotherms and pore size distribution, NMR, elemental analysis, TGA, and UV-vis spectroscopy please see the supplementary information.

References

1 J. L. Rowsell and O. M. Yaghi, *Journal of the American Chemical Society*, 2006, **128**, 1304-1315;M. Dincă, W. S. Han, Y. Liu, A. Dailly, C. M. Brown and J. R. Long, *Angewandte Chemie International Edition*, 2007, **46**, 1419-1422;K. L. Mulfort and J. T. Hupp, *Journal of the American Chemical Society*, 2007, **129**, 9604-9605;Y. Liu, J. F. Eubank, A. J. Cairns, J. Eckert, V. C. Kravtsov, R. Luebke and M. Eddaoudi, *Angewandte Chemie International Edition*, 2007, **46**, 3278-3283;H. Hayashi,

A. P. Cote, H. Furukawa, M. O'Keeffe and O. M. Yaghi, *Nature materials*, 2007, **6**, 501-506;P. L. Llewellyn, S. Bourrelly, C. Serre, A. Vimont, M. Daturi, L. Hamon, G. De Weireld, J.-S. Chang, D.-Y. Hong and Y. Kyu Hwang, *Langmuir*, 2008, **24**, 7245-7250;R. Banerjee, A. Phan, B. Wang, C. Knobler, H. Furukawa, M. O'Keeffe and O. M. Yaghi, *Science*, 2008, **319**, 939-943;S.-H. Cho, T. Gadzikwa, M. Afshari, S. T. Nguyen and J. T. Hupp, *European Journal of Inorganic Chemistry*, 2007, **2007**, 4863-4867;P. Horcajada, C. Serre, M. Vallet-Regí, M. Sebban, F. Taulelle and G. Férey, *Angewandte Chemie International Edition*, 2006, **45**, 5974-5978;M. H. Alkordi, Y. Liu, R. W. Larsen, J. F. Eubank and M. Eddaoudi, *Journal of the American Chemical Society*, 2008, **130**, 12639-12641.

2 M. Eddaoudi, D. B. Moler, H. Li, B. Chen, T. M. Reineke, M. O'keeffe and O. M. Yaghi, *Accounts of Chemical Research*, 2001, **34**, 319-330;M. Eddaoudi, J. Kim, N. Rosi, D. Vodak, J. Wachter, M. O'Keeffe and O. M. Yaghi, *Science*, 2002, **295**, 469-472;G. Férey, C. Mellot-Draznieks, C. Serre and F. Millange, *Accounts of chemical research*, 2005, **38**, 217-225;B. Moulton and M. J. Zaworotko, *Chemical Reviews*, 2001, **101**, 1629-1658;S. Kitagawa, R. Kitaura and S. i. Noro, *Angewandte Chemie International Edition*, 2004, **43**, 2334-2375;M. H. Alkordi, J. A. Brant, L. Wojtas, V. C. Kravtsov, A. J. Cairns and M. Eddaoudi, *Journal of the American Chemical Society*, 2009, **131**, 17753-17755.

3 A. P. Cote, A. I. Benin, N. W. Ockwig, M. O'Keeffe, A. J. Matzger and O. M. Yaghi, *science*, 2005, **310**, 1166-1170;R. W. Tilford, W. R. Gemmill, H.-C. zur Loye and J. J. Lavigne, *Chemistry of materials*, 2006, **18**, 5296-5301;H. M. El-Kaderi, J. R. Hunt, J. L. Mendoza-Cortés, A. P. Côté, R. E. Taylor, M. O'Keeffe and O. M. Yaghi, *Science*, 2007, **316**, 268-272;A. P. Cote, H. M. El-Kaderi, H. Furukawa, J. R. Hunt and O. M. Yaghi, *Journal of the American Chemical Society*, 2007, **129**, 12914-12915;J. R. Hunt, C. J. Doonan, J. D. LeVangie, A. P. Côté and O. M. Yaghi, *Journal of the American Chemical Society*, 2008, **130**, 11872-11873;P. Kuhn, M. Antonietti and A. Thomas, *Angewandte Chemie International Edition*, 2008, **47**, 3450-3453;N. A. Zwaneveld, R. Pawlak, M. Abel, D. Catalin, D. Gigmes, D. Bertin and L. Porte, *Journal of the American Chemical Society*, 2008, **130**, 6678-6679;E. L. Spitler and W. R. Dichtel, *Nature chemistry*, 2010, **2**, 672-677;N. L. Campbell, R. Clowes, L. K. Ritchie and A. I. Cooper, *Chemistry of Materials*, 2009, **21**, 204-206;M. H. Weston, O. K. Farha, B. G. Hauser, J. T. Hupp and S. T. Nguyen, *Chemistry of Materials*, 2012, **24**, 1292-1296.

4 D. Wu, F. Xu, B. Sun, R. Fu, H. He and K. Matyjaszewski, *Chemical reviews*, 2012, **112**, 3959-4015.

5 A. Stein, S. W. Keller and T. E. Mallouk, *Science*, 1993, **259**, 1558-1564;G. Férey, *Journal of Solid State Chemistry*, 2000, **152**, 37-48.

6 G. J. McManus, Z. Wang, D. A. Beauchamp and M. J. Zaworotko, *Chemical Communications*, 2007, 5212-5213;J. F. Eubank, F. Nouar, R. Luebke, A. J. Cairns, L. Wojtas, M. Alkordi, T. Bousquet, M. R. Hight, J. Eckert, J. P. Embs, P. A. Georgiev and M. Eddaoudi, *Angewandte Chemie International Edition*, 2012, **51**, 10099-10103;M. O'Keeffe, M. A. Peskov, S. J. Ramsden and O. M. Yaghi, *Accounts of chemical research*, 2008, **41**, 1782-1789;N. W. Ockwig, O. Delgado-Friedrichs, M. O'Keeffe and O. M. Yaghi, *Accounts of chemical research*, 2005, **38**, 176-182.

7 H. Deng, C. J. Doonan, H. Furukawa, R. B. Ferreira, J. Towne, C. B. Knobler, B. Wang and O. M. Yaghi, *Science*, 2010, **327**, 846-850.

8 M. K. Bhunia, K. Yamauchi and K. Takanabe, *Angewandte Chemie International Edition*, 2014, **53**, 11001-11005.

9 J. X. Jiang, F. Su, A. Trewin, C. D. Wood, N. L. Campbell, H. Niu, C. Dickinson, A. Y. Ganin, M. J. Rosseinsky and Y. Z. Khimyak, *Angewandte Chemie International Edition*, 2007, **46**, 8574-8578;J.-X. Jiang, F. Su, A. Trewin, C. D. Wood, H. Niu, J. T. Jones, Y. Z. Khimyak and A. I. Cooper, *Journal of the American Chemical Society*, 2008, **130**, 7710-7720.

10 R. Dawson, A. I. Cooper and D. J. Adams, *Progress in Polymer Science*, 2012, **37**, 530-563.

11 C. D. Wood, B. Tan, A. Trewin, F. Su, M. J. Rosseinsky, D. Bradshaw, Y. Sun, L. Zhou and A. I. Cooper, *Advanced Materials*, 2008, **20**, 1916-1921.

12 A. K. Sekizkardes, T. İslamoğlu, Z. Kahveci and H. M. El-Kaderi, *Journal of Materials Chemistry A*, 2014, **2**, 12492-12500;C. Xu, Z. Bacsik and N. Hedin, *Journal of Materials Chemistry A*, 2015, **3**, 16229-16234.

13 T. Ben, C. Pei, D. Zhang, J. Xu, F. Deng, X. Jing and S. Qiu, *Energy & Environmental Science*, 2011, **4**, 3991-3999.

14 R. Dawson, A. Laybourn, R. Clowes, Y. Z. Khimyak, D. J. Adams and A. I. Cooper, *Macromolecules*, 2009, **42**, 8809-8816;W. Lu, J. P. Sculley, D. Yuan, R. Krishna, Z. Wei and H. C. Zhou, *Angewandte Chemie International Edition*, 2012, **51**, 7480-7484;R. Dawson, D. J. Adams and A. I. Cooper, *Chemical Science*, 2011, **2**, 1173-1177;R. Dawson, A. I. Cooper and D. J. Adams, *Polymer International*, 2013, **62**, 345-352.

15 V. Guillerm, Ł. J. Weseliński, M. Alkordi, M. I. H. Mohideen, Y. Belmabkhout, A. J. Cairns and M. Eddaoudi, *Chemical Communications*, 2014, **50**, 1937-1940.